Formation of Highly Oxidized Radicals and Multifunctional Products from the Atmospheric Oxidation of Alkylbenzenes

Sainan Wang,[1,3] Runrun Wu,[1] Torsten Berndt,[2] Mikael Ehn,[3] and Liming Wang[1,4*]*

[1] School of Chemistry & Chemical Engineering, South China University of Technology, Guangzhou 510640, China.

[2] Leibniz Institute for Tropospheric Research, TROPOS, 04318 Leipzig, Germany

[3] Department of Physics, University of Helsinki, P.O. Box 64, Helsinki 00014, Finland

[4] Guangdong Provincial Key Laboratory of Atmospheric Environment and Pollution Control, South China University of Technology, Guangzhou 510006, China.

AUTHOR INFORMATION

Corresponding Author

Liming Wang, Email: wanglm@scut.edu.cn

Torsten Berndt, Email: berndt@tropos.de

ABSTRACT Aromatic hydrocarbons contribute significantly to tropospheric ozone and secondary organic aerosols (SOA). Despite large efforts in elucidating the formation mechanism of aromatic-derived SOA, current models still substantially underestimate the SOA yields when comparing to field measurements. Here we present a new, up to now undiscovered pathway for the formation of highly oxidized products from the OH-initiated oxidation of alkyl benzenes based on theoretical and experimental investigations. We propose that unimolecular H-migration followed by O_2-addition, a so-called autoxidation step, can take place in bicyclic peroxy radicals (BPRs), which are important intermediates of the OH-initiated oxidation of aromatic compounds. These autoxidation steps lead to the formation of highly oxidized multifunctional compounds (HOMs), which are able to form SOA. Our theoretical calculations suggest that the intramolecular H-migration in BPRs of substituted benzenes could be fast enough to compete with bimolecular reactions with HO_2 radicals or NO under atmospheric conditions. The theoretical findings are experimentally supported by flow tube studies using chemical ionization mass spectrometry to detect the highly oxidized peroxy radical intermediates and closed-shell products. This new unimolecular BPR route to form HOMs in the gas phase enhances our understanding of the aromatic oxidation mechanism, and contributes significantly to a better understanding of aromatic-derived SOA in urban areas.

KEYWORDS: Highly Oxidized Multifunctional Products; Bicyclic Peroxy Radicals; Unimolecular Hydrogen Migration; Mass Spectrometry

37 **TOC GRAPHICS**

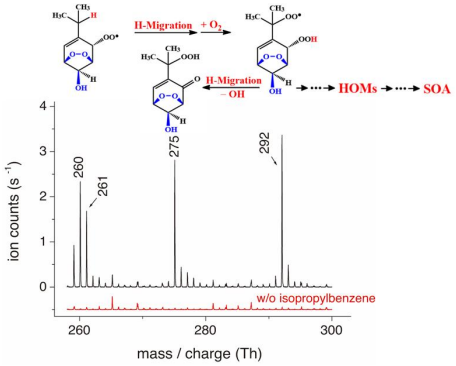

38

39

Introduction

Aromatic compounds represent an important fraction of the total volatile organic compounds in the urban atmosphere and play an important role in the formation of both tropospheric ozone and secondary organic aerosols (SOAs).[1-5] Typical anthropogenic sources of aromatic compounds include on-road vehicles, solvent usage, and industrial emissions. In industrialized regions of developing countries like China, serious pollutions from BTEX (Benzene, Toluene, Ethylbenzene, and Xylenes) were observed in winter due to coal combustion, e.g., BTEX concentrations were usually ~30 μg m^{-3} (1μg m^{-3} ~ 7.5 × 10^9 molecules cm^{-3} ~ 0.3 ppbv) or higher in non-haze days and could easily exceed 100 μg m^{-3} in haze days in northern China[6, 7] and other regions.[8, 9]

In the troposphere, oxidation of aromatic compounds is initiated by their reactions with OH radicals *via* H-abstraction from the alkyl groups and, more importantly, *via* OH addition to the aromatic ring, followed by further reactions to form bicyclic peroxy radicals (BPRs) (**Scheme 1**).[1, 10, 11] Based on the current mechanistic understanding, BPRs react with HO_2 radicals forming bicyclic hydroxyhydroperoxides (ROOH) as the main product under low-NO_x conditions. The reaction with NO yields bicyclic organic nitrates ($RONO_2$) as well as the corresponding bicyclic oxy radicals that finally form carbonylic products, such as (methyl) glyoxal, and other SOA precursors.[12-14] As a result of a smog chamber study on the oxidation of benzene, toluene, and xylene, it was found that SOA yields under low-NO_x conditions were higher than those obtained under high-NO_x conditions, presumably due to the formation of high yields of ROOHs from the reactions of BPRs with HO_2 radicals.[15] The bimolecular reactions of BPRs with HO_2 and NO have been incorporated into SOA formation models,[16-18] which, however, still underestimated the

SOA formation from xylene and toluene under both high-NO_x and low-NO_x conditions.[17, 18] The discrepancy between field measurements and modeling studies might suggest an alternative pathway of SOA formation from BPRs without the participation of HO_2 or NO.

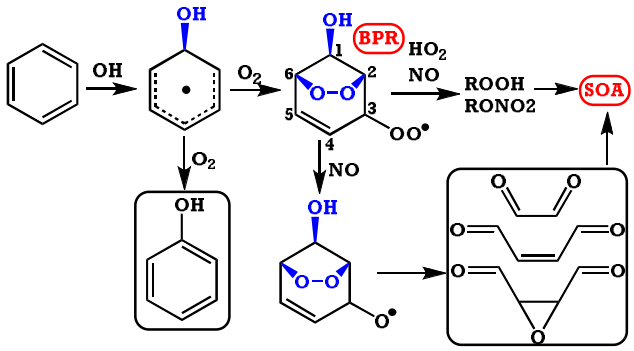

SCHEME 1. Main oxidation routes of benzene

Here we suggest an alternative reaction pathway of BPRs that starts with an unimolecular isomerization step of BPRs being competitive with the bimolecular BPR reaction, e.g. at 0.1 – 10 s^{-1} with NO in the range of 0.4 – 40 ppbv or at ~0.01 s^{-1} with HO_2 of 40 pptv and the bimolecular rate coefficients of ~1 × 10^{-11} cm^3 $molecule^{-1}$ s^{-1}.[19] Our recent theoretical study on the oxidation of benzyl alcohol showed that the intramolecular H-migrations of the corresponding BPRs proceed with rate coefficients of ~10 s^{-1} at 298 K.[20] Fast H-migrations under atmospheric conditions were also found for peroxy radicals formed in the oxidation of a series of important organic precursor compounds,[21-29] resulting in the formation of highly oxidized multifunctional compounds (HOMs). Particularly, fast H-migration might partially account for the recently observed HOMs with an O:C ratio up to 1.09 in the OH-initiated oxidation of benzenes.[30] Given the importance of alkylbenzenes in the urban atmosphere, we investigated here the role of H-migrations of BPRs from the oxidation of aromatic compounds using toluene (**T**), ethylbenzene (**EB**), and isopropylbenzene (**IB**) as the model substances.

Theoretical and Experimental Methods

Theoretical Methods All molecular structures were optimized at DFT-M06-2X/6-311++G(2df, 2p) level which has been assessed to be suitable for thermokinetic studies.[31] The optimized structures were submitted to electronic energies using restricted open-shell complete basis set model chemistry (ROCBS-QB3)[32] which uses the spin-restricted wave functions to eliminate the need for empirical correction for spin contamination in UCBS-QB3. Values of the T1 diagnostic in ROCCSD/6-31+G(d') calculations were used to check the multireference characteristic of the wavefunctions. Generally, a T1 diagnostic larger than 0.02 suggests a multireference nature of the wavefunction,[33, 34] but Olivella et al. also found that RCCSD(T) agreed well with the multireference method CASPT2 in the calculations of benzene oxidation when the T1 diagnostic is less than 0.044.[35] In this work, we found that the T1 diagnostics were all less than 0.03 for the transition states of critical steps, indicating the reliability of our calculations. All the quantum chemical calculations were carried out using the Gaussian 09 package.[36]

The reaction rate coefficients of the unimolecular reactions were calculated using the unimolecular rate theory coupled with the energy-grained master equation for collisional energy transfer (RRKM-ME),[37, 38] and the rate coefficients of bimolecular reactions were determined using traditional transition state theory.[39, 40] The RRKM-ME calculations were carried out using the Mesmer code.[41] A single exponential-down model was used to approximate the collisional energy transfer with $<\Delta E>_{down}$ of 200 cm^{-1}. The collisional parameters were estimated using the method of Gilbert and Smith,[42] and the asymmetric Eckart model was used for the tunneling correction factors.[43] With the uncertainty in barrier heights (~4 kJ/mol by ROCBS-QB3) and in

tunneling correction factors, we estimate an uncertainty of about one order of magnitude for the unimolecular rates at 298 K.

Experimental Methods The experimental studies were performed in a free-jet flow system at a temperature of 295 ± 2 K, a pressure of 1 bar air and a reaction time of 7.9 s.[44, 45] The detection of highly oxidized peroxy radicals and closed-shell products was carried out by means of CI-APi-TOF (chemical ionization - atmospheric pressure interface - time-of-flight) mass spectrometry (Airmodus, Tofwerk, resolving power >3000 Th/Th) at atmospheric pressure using acetate as the reagent ion.[44-47] The stated concentrations represent estimated lower end values assuming efficient clustering of acetate ions with the highly oxidized products with a rate coefficient at the collision limit.[44, 45] This experimental approach allows following the early, highly oxidized products, including peroxy radicals, with a detection limit as low as 10^4 molecules cm^{-3}. OH radicals were generated via ozonolysis of tetramethylethylene. Calculated steady-state OH concentrations were in the range (2.4 - 53) × 10^4 molecules cm^{-3}. More experimental information is given in Supporting Information.

Results and Discussion

OH addition to **T**, **EB**, and **IB** forms four different adducts, denoted as R1-R4 for additions to *ipso*-, *ortho*-, *meta*-, and *para*-positions, respectively, resulting after two subsequent O_2 additions in the formation of the corresponding BPRs in alkyl benzenes.[11, 20, 48-51] Calculations showed that the first O_2 adds to the aromatic ring from the same direction as the OH radical (*syn*), while the second O_2 adds from the opposite direction relative to OH group (*anti*). BPRs are therefore denoted as R*n*-*ij*OO-*s*-*k*OO-*a*, in which *n* is the site of OH addition, *i* and *j* are the sites connecting the –OO– unit, and *k* is the site of the second O_2 addition, and *a*/*s* is *anti*/*syn* (*see*

Scheme 1 for the numbering of sites). Additions of OH to *meta*-position are usually ignored because of their small branching ratios. The radicals R1-26OO-*s*-3OO-*a*, R2-13OO-*s*-6OO-*a* and R4-35OO-*s*-2OO-*a* can possibly undergo intramolecular H-migrations as shown in **Scheme 2**, resulting in another set of peroxy radicals O_2QOOH (HO-Ar-$(O_2)_3$, denoted as R1-QP, R2-QPH2 and R4-QP1/R4-QP2) after the third O_2 addition. H-migration channel is not available to R2-13OO-s-4OO-a, which could also be formed from R2 channel.

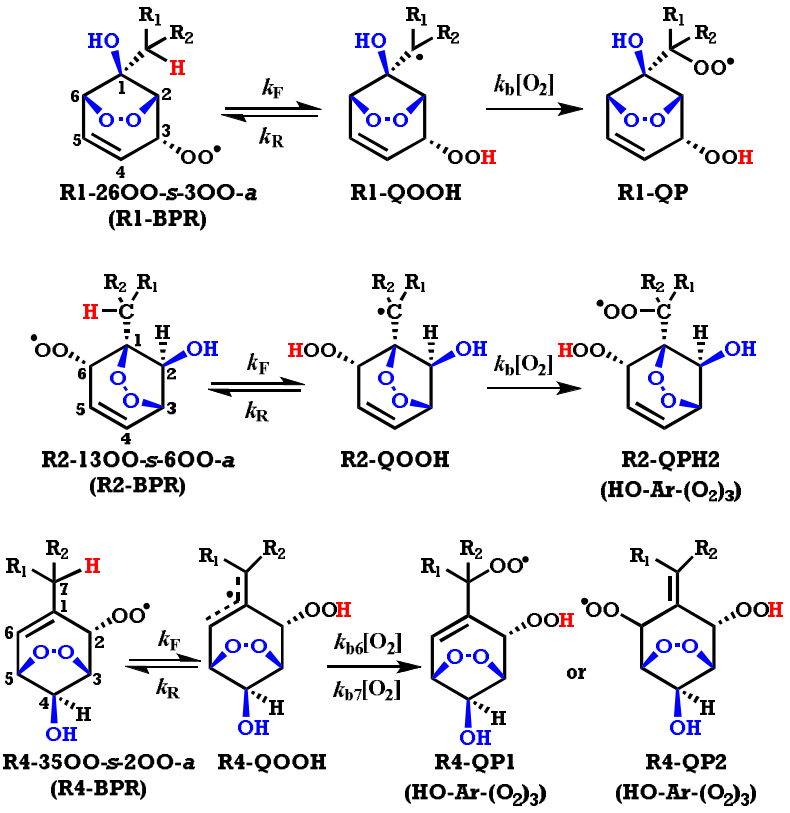

Scheme 2. H-migrations in bicyclic peroxy radicals (*a*/*s* = *anti*/*syn* represents the direction of –OO– or –OO relative to –OH group)

Theoretical Results In order to probe the feasibility of the proposed H-migrations, we first estimated their rate coefficients using quantum chemistry calculations and the unimolecular rate theory (RRKM-ME). The results are listed in Table 1. All H-migrations in R1-BPRs and R2-

BPRs are endothermic and therefore highly reversible. H-migrations in R4-BPRs are about thermal neutral due to the conjugated π-bond in the radical products and fast recombination of R4-QOOH with O_2, and are therefore virtually irreversible. Barrier heights for H-migrations are reduced by 9 - 20 kJ/mol upon successive methyl substitution from **T** to **EB** and to **IB**, and barrier heights in R4-BPRs are much lower than those in R1- and R2-BPRs. The lower barriers and irreversibility for R4-BPRs imply the importance or even the dominance of H-migration under atmospheric conditions for these radicals. For O_2 addition to R4-QOOH, calculations show that radicals R4-QP1 and R4-QP2 are formed with branching ratios of 0.67 and 0.33 for **T**, 0.19 and 0.81 for **EB**, and 0.56 and 0.44 for **IB**, respectively, at 298 K.

Each bicyclic peroxy radical has multiple conformers due to internal rotations, of which the internal rotations of the alkyl groups and the –OO group are frozen in transition states for H-migrations. Therefore, we have paid special attention to identify the lowest energy conformer for each bicyclic peroxy radical by rotating all the rotatable bonds. In the kinetics calculations, we have also treated the two internal rotations as two uncoupled hindered rotors, and have obtained their potential energy profiles by fixing the corresponding dihedral angles while relaxing all other coordinates in optimization. The potential energy profiles are shown in Figures S1-S3 in the Supporting Information. The unimolecular rate coefficients obtained are listed in Table 1. Discussions below were based on rates predicted with consideration of internal rotations.

Assuming steady state conditions for QOOH led to the effective rate coefficients $k_{\mathrm{b,Eff}}$ (in s^{-1}) from BPRs to QPs *via* H-migration as

$$k_{\mathrm{b,Eff}} = \frac{k_{\mathrm{F}} k_{\mathrm{b}} [\mathrm{O_2}]}{k_{\mathrm{R}} + k_{\mathrm{b}} [\mathrm{O_2}]}$$

Table 1. Reaction energies and barrier heights (ΔE_{0K} and $\Delta E_{0K}^{\neq}$, in kJ/mol) at ROCBS-QB3 level, the rates at 298 K and T-dependence rate coefficients (k_F, k_R, and $k_{b,Eff}$, all in s^{-1}) for the intramolecular H-migrations in BPRs

BPRs	ΔE_{0K}	$\Delta E_{0K}^{\neq}$	k_F [a]	k_R [a]	$k_{b,Eff}$ [a]	k_F [b]	k_R [b]	$k_{b,Eff}$ [b]
T-R1-	65.2	110.1				5.2×10^{-6}	1.9×10^{6}	5.1×10^{-6}
						$\ln k_{b,Eff}(T) = 18.77 - 9.11\times10^{3}/T$		
T-R2-	67.8	101.8				5.2×10^{-5}	2.8×10^{8}	8.0×10^{-6}
						$\ln k_{b,Eff}(T) = 16.37 - 8.37\times10^{3}/T$		
T-R4-	12.5	93.2				2.6×10^{-2}	2.6×10^{1}	2.6×10^{-2}
						$\ln k_{b,Eff}(T) = 9.67 - 3.92\times10^{3}/T$		
EB-R1-	52.2	92.1	1.3×10^{-2}	5.1×10^{6}	1.2×10^{-2}			
	52.2	94.2	1.0×10^{-2}	3.7×10^{6}	9.4×10^{-3}			
			$\ln k_{b,Eff}(T) = 23.54 - 7.37\times10^{3}/T$					
EB-R2-	53.3	85.8	1.0×10^{-2}	3.7×10^{6}	1.6×10^{-2}	1.2×10^{-2}	2.0×10^{8}	2.5×10^{-3}
			$\ln k_{b,Eff}(T) = 18.32 - 6.69\times10^{3}/T$			$\ln k_{b,Eff}(T) = 16.24 - 6.63\times10^{3}/T$		
EB-R4-	–3.9	76.8	4.2×10^{1}	8.9×10^{0}	4.2×10^{1}	7.0	8.9	7.0
			$\ln k_{b,Eff}(T) = 13.00 - 2.71\times10^{3}/T$			$\ln k_{b,Eff}(T) = 10.167 - 2.40\times10^{3}/T$		
IB-R1-	51.3	81.3	4.5×10^{-1}	6.1×10^{7}	2.0×10^{-1}			
			$\ln k_{b,Eff}(T) = 21.17 - 6.78\times10^{3}/T$					
IB-R2-	31.3	70.2	6.7×10^{1}	6.6×10^{6}	5.9×10^{1}	21	6.7×10^{6}	8.8
			$\ln k_{b,Eff}(T) = 21.29 - 5.11\times10^{3}/T$			$\ln k_{b,Eff}(T) = 17.34 - 4.51\times10^{3}/T$		
IB-R4-	–7.7	67.6	4.7×10^{2}	3.2×10^{1}	4.7×10^{2}	14	33	14
			$\ln k_{b,Eff}(T) = 14.65 - 2.49\times10^{3}/T$			$\ln k_{b,Eff}(T) = 11.32 - 2.53\times10^{3}/T$		
T-R1-QP		149.2						$< 10^{-8}$ (298 K)
		132.0						$< 10^{-8}$ (298 K)
T-R2-QP		93.3						1.1×10^{-2} (298 K)
T-R4-QP		84.0						~ 8 (298 K)
EB-R4-QP2-s		83.0						~0.6 (298 K)
IB-R4-QP2-s		79.4						~16 (298 K)

[a] Treating internal rotations as hindered rotors; [b] Treating internal rotation as harmonic oscillators

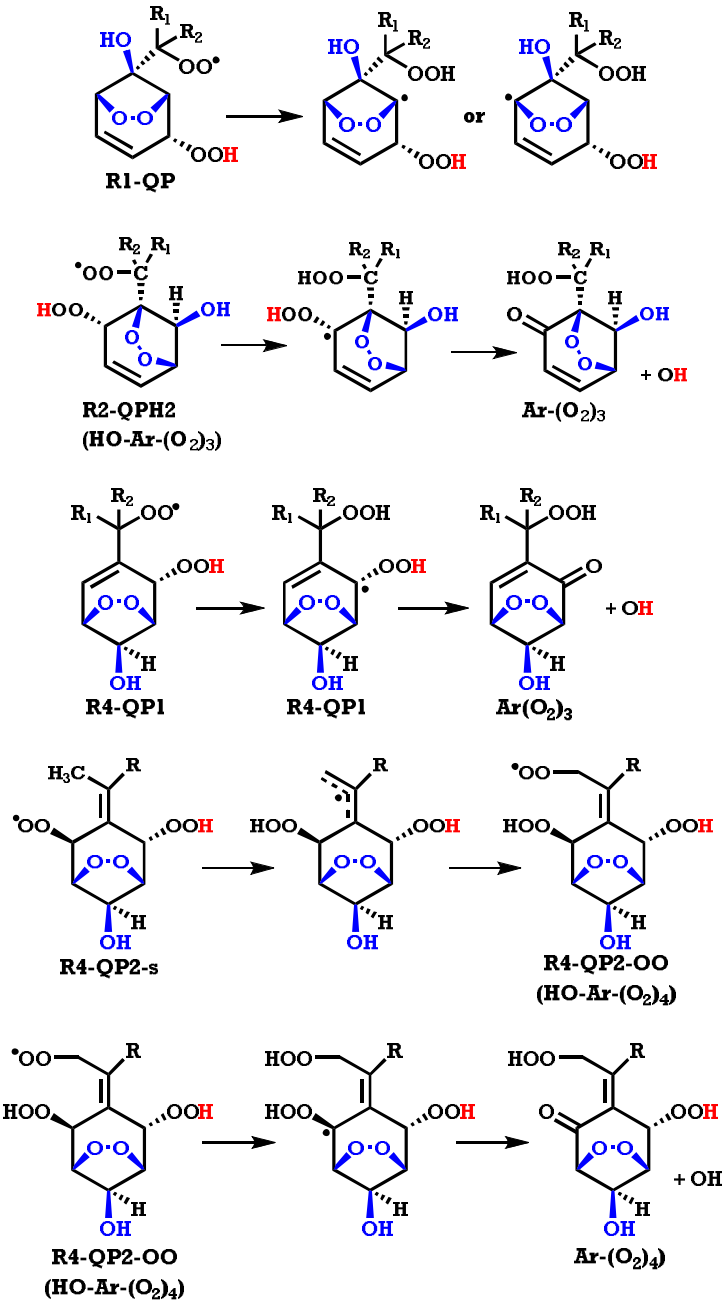

Scheme 3. H-migrations in R1-QP, R2-QPH2, and R4-QP1/-QP2

where k_F, k_R, and $k_b[O_2]$ are defined in **Scheme 2**. We have estimated $k_{b,Eff}$ using our calculated values for k_F and k_R (see Table 1) and $k_b = 10^{-11}$ cm^3 molecule^{-1} s^{-1} for a temperature range of 243 - 333 K[52] and $[O_2] = 5 \times 10^{18}$ molecules cm^{-3}. The results are also included in Table 1. The results clearly showed that H-migration in BPRs could be important under typical atmospheric

conditions except for **T**-R1- and **T**-R2-BPR. The estimated $k_{b,Eff,298K}$'s of ~7 s^{-1}, ~9 s^{-1}, and ~14 s^{-1} in **EB**-R4-, **IB**-R2-, and **IB**-R4-BPRs, respectively, are higher than or comparable to the possible pseudo first-order rate coefficients of 0.1 – 10^{-1} s for the bimolecular removals with NO of 0.4 – 40 ppbv or ~0.01 s^{-1} with HO_2 radicals of 40 pptv in the atmosphere, suggesting the importance of H-migration in BPRs even in the highly polluted atmosphere. H-migration in **T**-R4-BPR with $k_{b,Eff,298K}$ of ~0.02 s^{-1} could be comparable to the bimolecular removals when NO/HO_2 concentrations are low in remote areas and even in the urban atmosphere in the afternoon (NO concentrations < 1 ppbv).[53] Expectedly, the H-migration becomes faster at high temperatures and slower at low temperatures. It should be still important even in the cold winter with $k_{b,Eff,263K}$ of ~2.5 s^{-1}, 1.2 s^{-1}, and 4.7 s^{-1} for **EB**-R4-, **IB**-R2-, and **IB**-R4-BPRs.

The R2-QPH2 and R4-QP1 radicals formed from H-migration of BPRs might undergo another H-migration (**Scheme 3**). We have obtained barriers of 93.3 and 84.0 kJ/mol for H-migrations in **T**-R2-QPH2 and **T**-R4-QP1 and estimated rate coefficients of ~1.1 × 10^{-2} and ~8 s^{-1} at 298 K. The H-migrations in **T**-R1-QP would be too slow because of high barriers of > 130 kJ/mol. For EB and IB, the R4-QP2 radicals could undergo a different H-migration from the methyl group with barriers of only 83.0 kJ/mol and 79.4 kJ/mol. Radicals R4-QP2-OO as HO-Ar-$(O_2)_4$ are followed by the addition of the fourth O_2. A third H-migration in R4-QP2-OO is also possible in analogy to that in R4-BPRs (**Scheme 3**). It should be noted here that the barrier heights might be over-estimated because the T1 diagnostics in ROCCSD calculations of these transition states were higher than 0.05. Similar effective rate coefficients for **EB-** and **IB**-QPs are expected because methyl substitution would have a small effect on the barrier height (might be slightly smaller due to the increased size of the radicals). HOMs are formed as $Ar(O_2)_3$ isomers

from both R2-QPH2 and R4-QP1s and $Ar(O_2)_4$ from R4-QP2, all with a recycling of OH radicals.

The theoretical results here suggested potential formation pathways for highly oxygenated HO-Ar-$(O_2)_3$ radicals as R4-QP1 and R4-QP2 in **T** and as all possible QPs in **EB** and **IB** via the first H-migration in BPRs (**Scheme 2**), as well as the formation of the corresponding closed-shell HOMs as Ar-$(O_2)_3$ (from R2-QPs and R4-QP1) after a second H-migration (**Scheme 3**). In the atmosphere, radicals HO-Ar-$(O_2)_3$ would also react with NO and HO_2 radicals forming organic nitrates, hydroperoxide moiety-containing HOMs, and others.[52]

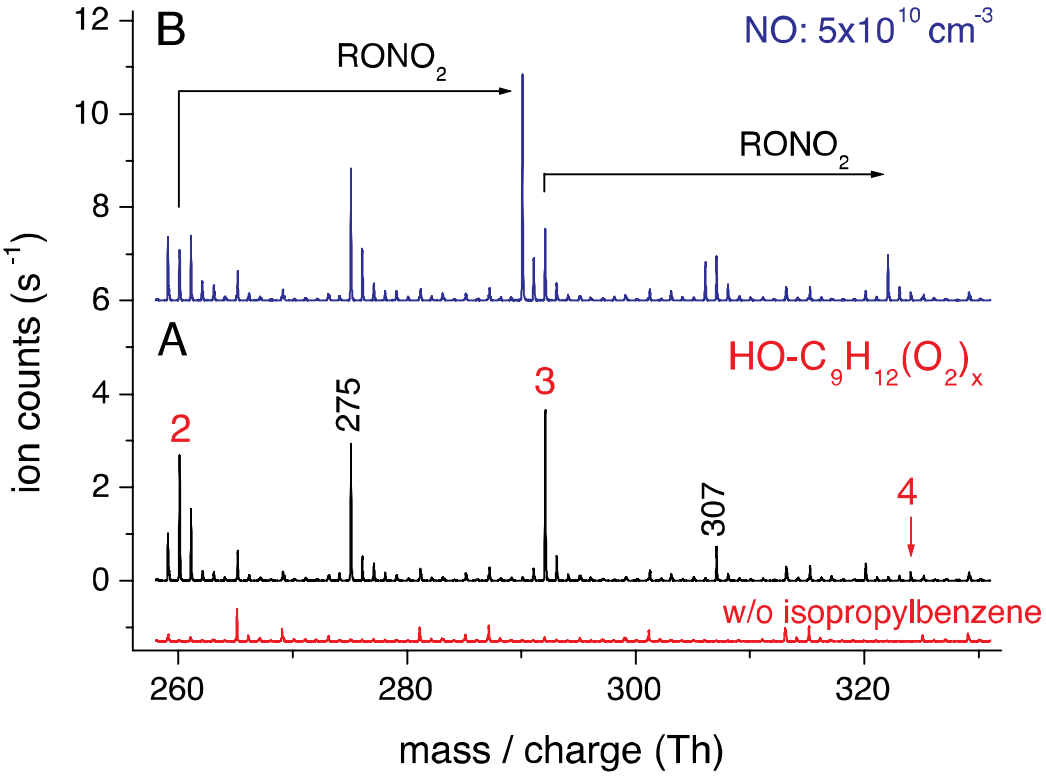

Figure 1. Mass spectra recorded from the reaction of OH radicals with isopropylbenzene, **IB**. The red spectrum represents the background measured in absence of isopropylbenzene. Products are detected as adduct with acetate. The spectrum depicted in part A was measured in absence of NO and that in part B with a NO concentration of 5×10^{10} molecules cm^{-3}. Reactant concentrations (unit: molecules cm^{-3}): $[O_3] = 6.6 \times 10^{11}$, [TME] = 1.0×10^{11} and [isopropylbenzene] = 1.64×10^{13}.

Experimental Results The predicted formation of highly oxidized radicals and closed-shell products having undergone multiple H-migration steps was further investigated in a flow tube reactor. At the low radical concentrations and short reaction times (7.9 s) used, bimolecular reactions between radicals are negligible and any detected highly oxidized RO_2 radicals should arise dominantly from unimolecular pathways. Low radical concentrations suggest negligible reactions between BPRs and between BPRs and other peroxy radicals or HO_2 radicals.

Figure 1A shows a measured mass spectrum during an experiment where **IB** was oxidized by OH radicals. Signals at nominal mass-to-charge ratios 260, 292 and 324 Th were attributed to the acetate adducts of RO_2 radicals with chemical formula $HO\text{-}C_9H_{12}\text{-}(O_2)_x$ with x = 2, 3 and 4, respectively. The radicals with x = 2 would thus correspond to BPRs, those with x = 3 to R2-QPH2 and R4-QP1/QP2, and those with x = 4 to R4-QP2-OO in **Schemes 2 and 3**. Signals at 275 and 307 Th can correspond to the closed-shell products arising from the RO_2 radicals with x = 3 and 4, respectively, after formal loss of one -OH group (-17 Th). The signals at 275 Th and 307 Th are consistent with the products $Ar\text{-}(O_2)_3$ and $Ar\text{-}(O_2)_4$, i.e. $C_9H_{12}\text{-}(O_2)_3$ and $C_9H_{12}\text{-}(O_2)_4$ in **IB** in **Scheme 3**.

Experiments in the presence of NO were carried out in order to test for the functionality of the supposed RO_2 radicals by measuring the corresponding organic nitrates formed via $RO_2 + NO \rightarrow RONO_2$. Figure 1B clearly illustrates the occurrence of the expected nitrates from the RO_2 radicals with x = 2 and 3 for [NO] of 5×10^{10} molecules cm^{-3}, strongly supporting the identification of highly oxidized RO_2 radicals. Moreover, H/D exchange experiments with D_2O have been performed to identify the number of acidic H atoms in the products, i.e. the total number of HO- and HOO-groups.[54] Figures S4a and S4b show mass spectra from the reaction of

OH radicals with **IB** recorded in absence and presence of D_2O, respectively. According to that, the RO_2 radical HO-$C_9H_{12}(O_2)_x$ with x = 2 (BPRs) contains only one acidic H-atom, very likely the HO-group from the attacking OH radical on the aromatic ring, being in line with the assumed BPR structure in **Scheme 2**. Two acidic H-atoms were found for the RO_2 radical with x = 3 and its corresponding closed-shell product formed after elimination of one OH group, consistent with the expected RO_2 radicals R2-QPH2 and R4-QP1/QP2 and closed-shell Ar-$(O_2)_3$, respectively, which either contain one HO- and one HOO-group or two HOO-groups (**Scheme 3**). Similarly, three acidic H-atoms were found for the RO_2 radical with x = 4 and closed-shell compounds after eliminating one OH group, consisting with the expected R4-QP2-OO and Ar-$(O_2)_4$ in **Scheme 3**. It should also be noted that the HO-Ar-$(O_2)_x$ intensities for x = 2 are most likely underestimated due to the presence of only one HO-group and the associated relatively low acetate-cluster stability, and better detection sensitivity is expected for the radicals with x = 3 and 4 as well as for the closed-shell products with x = 3 -17 Th due to the presence of a second functional group that enhances the cluster stability.[55]

Figure 2 shows a comparison of the detected RO_2 radicals and closed-shell HOMs from the OH radical reactions of benzene (part A) and **IB** (part B). The almost linear increase of the RO_2 radical concentrations with rising precursor conversion indicates the absence of significant bimolecular reactions with other RO_2 or HO_2 radicals. Low HO-$C_6H_6(O_2)_x$ with x = 3 and 4 from benzene is consistent with the extremely high barriers of more than 120 kJ/mol for H-migrations in BPR of benzene (Figure S5). The detection of the corresponding nitrates from HO-$C_6H_6(O_2)_x$ with x = 3 and 4 in benzene was impossible due to insufficient signal intensities. Results for toluene and ethylbenzene are given in Figures S6 and S7.

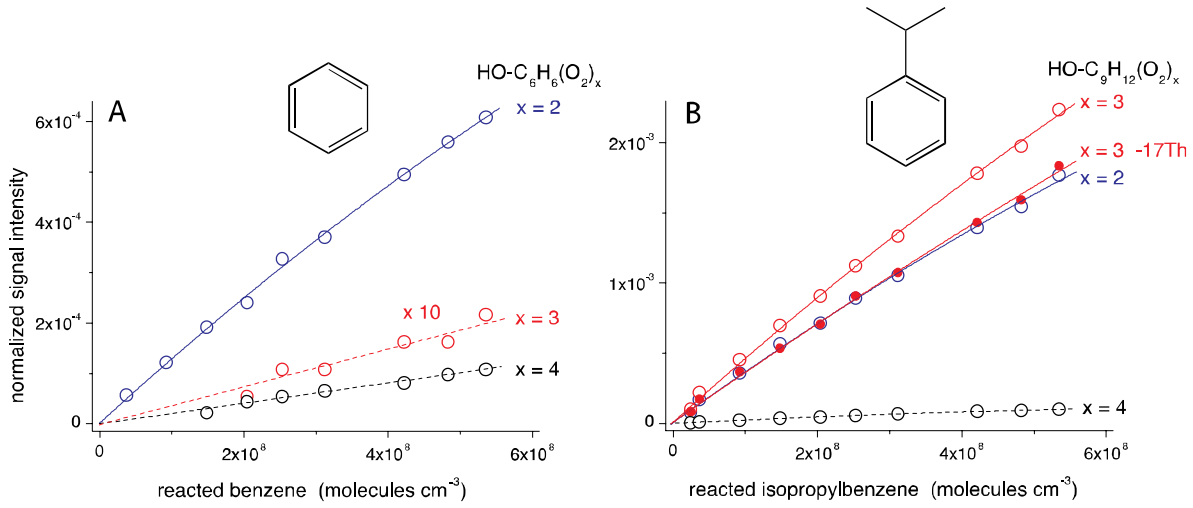

258

259 **Figure 2**. Signals attributed to RO_2 radical HO-aromatic$(O_2)_x$ for x = 2, 3 and 4 as a function of
260 reacted benzene (part **A**) and isopropylbenzene (part **B**). The closed-shell product formed from
261 the RO_2 radical with x = 3 (x = 3 -17 Th) is given in **B** as well. Reactant concentrations (unit:
262 molecules cm^{-3}): $[O_3]$ = (3.4 – 75) × 10^{10}, [TME] = 1.0 × 10^{11}, [benzene] = 1.0 × 10^{14} and
263 [isopropylbenzene] = 1.64 × 10^{13}. Organic nitrate detection for RO_2 radicals shown with a
264 dashed line was not successful caused by low signal intensity.

265

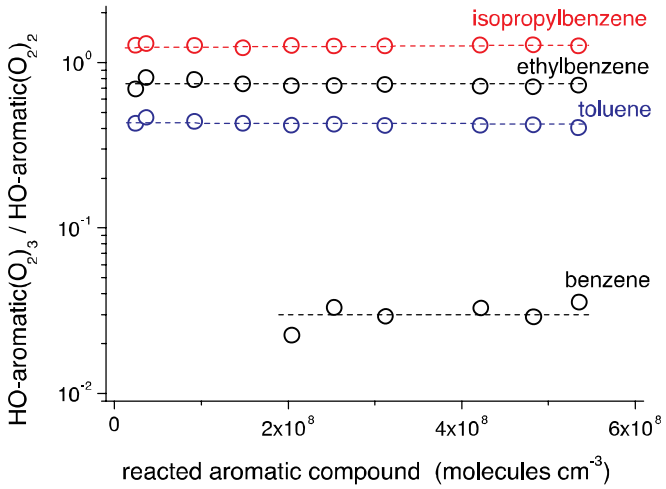

266

267 **Figure 3**. RO_2 radical concentrations HO-Ar-$(O_2)_x$ with x = 3 normalized by the RO_2
268 concentration for x = 2 observed from the reaction of OH radicals with benzene, toluene,
269 ethylbenzene and isopropylbenzene. The given ratio for the benzene system represents an upper
270 limit because of the large uncertainty of the HO-$(C_6H_6)(O_2)_3$ concentration.

The importance of alkyl substitution for the formation of highly oxidized RO_2 radicals becomes obvious from the comparison of the experimental results for the four aromatic compounds investigated (Figure 3). The ratio HO-Ar-$(O_2)_3$/HO-Ar-$(O_2)_2$ is independent of the amount of converted aromatic compound for all four reaction systems, being in line with the almost linear signal increase with rising precursor conversion as given in Figures 2, S5 and S6. The observed trend of the ratios is in accordance with the predicted overall rates of ~(8.8 – 14), ~7.0, and ~2.6×10^{-2} s^{-1} from BPRs (x = 2) to HO-Ar-$(O_2)_3$ for **IB**, **EB**, and **T**. Note that some HO-Ar-$(O_2)_2$ radicals have no H-migration channel, such as the R2-13OO-s-4OO-a, because no neighboring hydrogen is available in these structures.

Atmospheric Implication We have predicted theoretically and confirmed experimentally the occurrence of intramolecular H-migrations in BPRs formed in the atmospheric oxidation of **T, EB**, and **IB** and the subsequent formation of HOMs in gas phase. These HOMs should contribute significantly to the formation of SOA in urban areas. Earlier studies have shown the importance of HOMs in the OH-initiated oxidation of biogenic VOCs,[44] and we have now found that similar HOM formation pathways exist also for alkylbenzenes in the atmosphere. The recycling of OH radicals along with the gas-phase formation of Ar-$(O_2)_3$ from R2/R4-BPRs suggests a certain degree of autoxidation without the involvement of HO_2/NO. The role of H-migration might be more important in *m*-xylene, 1,2,4-trimethylbenzene, and 1,3,5-trimethylbenzene than in toluene because of the higher branching ratios of ~13%, ~27%, and >90% for R4 radicals than that of ~5% in toluene amongst the OH addition channels.[11, 48, 49]

ASSOCIATED CONTENT

Supporting Information. Details of theoretical and experimental methods, potential energy profiles for internal rotations, mass spectra, and potential energy diagram for Benzene-BPR. This material is available free of charge via the Internet at http://pubs.acs.org.

AUTHOR INFORMATION

Corresponding Authors

Liming Wang, Email: wanglm@scut.edu.cn, and Torsten Berndt, Email: berndt@tropos.de.

The authors declare no competing financial interests.

ACKNOWLEDGMENT

LW thanks for the financial supports from National Natural Science Foundation of China (No. 21477038) and Natural Science Foundation of Guangdong Province (No. 2016A030311005). SW thanks for the support from China Scholarship Council. This work was supported by the European Research Council (Grant 638703-COALA).

REFERENCES

1. Calvert, J. G.; Atkinson, R.; Becker, K. H.; Kamens, R. M.; Seinfeld, J. H.; Wallington, T. J.; Yarwood, G., *The Mechanisms of Atmospheric Oxidation of the Aromatic Hydrocarbons*. Oxford University Press: 2002.
2. Bloss, C.; Wagner, V.; Jenkin, M. E.; Volkamer, R.; Bloss, W. J.; Lee, J. D.; Heard, D. E.; Wirtz, K.; Martin-Reviejo, M.; Rea, G.; Wenger, J. C.; Pilling, M. J., Development of a Detailed Chemical Mechanism (MCMv3.1) for the Atmospheric Oxidation of Aromatic Hydrocarbons. *Atmos. Chem. Phys.* **2005,** *5*, 641-664.
3. Forstner, H. J. L.; Flagan, R. C.; Seinfeld, J. H., Secondary Organic Aerosol from the Photooxidation of Aromatic Hydrocarbons: Molecular Composition. *Environ. Sci. Technol.* **1997,** *31*, 1345-1358.
4. Odum, J. R.; Jungkamp, T. P. W.; Griffin, R. J.; Flagan, R. C.; Seinfeld, J. H., The Atmospheric Aerosol-Forming Potential of Whole Gasoline Vapor. *Science* **1997,** *276*, 96-99.
5. Offenberg, J. H.; Lewis, C. W.; Lewandowski, M.; Jaoui, M.; Kleindienst, T. E.; Edney, E. O., Contributions of Toluene and α-Pinene to SOA Formed in an Irradiated Toluene/α-Pinene/NO_x/Air Mixture: Comparison of Results Using ^{14}C Content and SOA Organic Tracer Methods. *Environ. Sci. Technol.* **2007,** *41*, 3972-3976.

6. Liu, K.; Zhang, C.; Cheng, Y.; Liu, C.; Zhang, H.; Zhang, G.; Sun, X.; Mu, Y., Serious BTEX Pollution in Rural Area of the North China Plain During Winter Season. *J. Environ. Sci.* **2015,** *30*, 186-190.
7. Zhang, Y.; Mu, Y.; Meng, F.; Li, H.; Wang, X.; Zhang, W.; Mellouki, A.; Gao, J.; Zhang, X.; Wang, S.; Chao, F., The Pollution Levels of BTEX and Carbonyls Under Haze and Non-haze Days in Beijing, China. *Sci. Total Environ.* **2014,** *490*, 391-396.
8. Cai, C.; Geng, F.; Tie, X.; Yu, Q.; An, J., Characteristics and Source Apportionment of VOCs Measured in Shanghai, China. *Atmos. Environ.* **2010,** *44*, 5005-5014.
9. Tang, J. H.; Chan, L. Y.; Chan, C. Y.; Li, Y. S.; Chang, C. C.; Wang, X. M.; Zou, S. C.; Barletta, B.; Blake, D. R.; Wu, D., Implication of changing urban and rural emissions on non-methane hydrocarbons in the Pearl River Delta region of China. *Atmos. Environ.* **2008,** *42*, 3780-3794.
10. Birdsall, A. W.; Andreoni, J. F.; Elrod, M. J., Investigation of the Role of Bicyclic Peroxy Radicals in the Oxidation Mechanism of Toluene. *J. Phys. Chem. A* **2010,** *114*, 10655-10663.
11. Wu, R.; Pan, S.; Li, Y.; Wang, L., Atmospheric Oxidation Mechanism of Toluene. *J. Phys. Chem. A* **2014,** *118*, 4533-4547.
12. Carlton, A. G.; Bhave, P. V.; Napelenok, S. L.; Edney, E. O.; Sarwar, G.; Pinder, R. W.; Pouliot, G. A.; Houyoux, M., Model representation of secondary organic aerosol in CMAQv4.7. *Environ. Sci. Technol.* **2010,** *44*, 8553-8560.
13. Carter, W. P. L.; Heo, G., Development of Revised SAPRC Aromatics Mechanisms. *Atmos. Environ.* **2013,** *77*, 404-414.
14. Hallquist, M.; Wenger, J. C.; Baltensperger, U.; Rudich, Y.; Simpson, D.; Claeys, M.; Dommen, J.; Donahue, N. M.; Geroge, C.; Goldstein, A. H.; Hamilton, J. F.; Herrmann, H.; Hoffmann, T.; Iinuma, Y.; Jang, M.; Jenkin, M. E.; Jimenez, J. L.; Kiendler-Scharr, A.; Maenhaut, W.; McFiggans, G.; Mental, T. F.; Monod, A.; Prevot, A. S. H.; Seinfeld, J. H.; Surratt, J. D.; Szmigielski, R.; Wildt, J., The formation, properties and impact of secondary organic aerosol: current and emerging issues. *Atmos. Chem. Phys.* **2009,** *9*, 5155-5236.
15. Ng, N. L.; Kroll, J. H.; Chan, A. W. H.; Chhabra, P. S.; Flagan, R. C.; Seinfeld, J. H., Secondary Organic Aerosol Formation from *m*-Xylene, Toluene, and Benzene. *Atmos. Chem. Phys.* **2007,** *7*, 3909-3922.
16. Henze, D. K.; Seinfeld, J. H.; Ng, N. L.; Kroll, J. H.; Fu, T.-M.; Jacob, D. J.; Heald, C. L., Global Modeling of Secondary Organic Aerosol Formation from Aromatic Hydrocarbons: High- vs. Low-Yield Pathways. *Atmos. Chem. Phys.* **2008,** *8*, 2405-2421.
17. Xu, J.; Griffin, R. J.; Liu, Y.; Nakao, S.; Cocker III, D. R., Simulated Impact of NO_x on SOA Formation from Oxidation of Toluene and m-Xylene. *Atmos. Environ.* **2015,** *101*, 217-225.
18. Dawson, M. L.; Xu, J.; Griffin, R. J.; Dabdub, D., Development of aroCACM/MPMPO 1.0: A Model to Simulate Secondary Organic Aerosol from Aromatic Precursors in Regional Models. *Geosci. Model Dev.* **2016,** *9*, 2143-2151.
19. Elrod, M. J., Kinetics Study of the Aromatic Bicyclic Peroxy Radical + NO Reaction: Overall Rate Constant and Nitrate Product Yield Measurements. *J. Phys. Chem. A* **2011,** *115*, 8125-8130.
20. Wang, L., The Atmospheric Oxidation Mechanism of Benzyl Alcohol Initiated by OH Radicals: The Addition Channels. *ChemPhysChem* **2015,** *16*, 1542-1550.
21. Rissanen, M. O.; Kurten, T.; Sipila, M.; Thornton, J. A.; Kangasluoma, J.; Sarnela, N.; Junninen, H.; Jorgensen, S.; Schallhart, S.; Kajos, M. K.; Taipale, R.; Springer, M.; Mentel, T.

F.; Ruuskanen, T.; Petaja, T.; Worsnop, D.; Kjaergaard, H. G.; Ehn, M., The Formation of Highly Oxidized Multifunctional Products in the Ozonolysis of Cyclohexene. *J. Am. Chem. Soc.* **2014,** *136*, 15596-15606.
22. Mentel, T. F.; Springer, M.; Ehn, M.; Kleist, E.; Pullinen, I.; Kurten, T.; Rissanen, M. O.; Wahner, A.; Wildt, J., Formation of Highly Oxidized Multifunctional Compounds: Autoxidation of Peroxy Radicals Formed in the Ozonolysis of Alkenes - Deduced from Structure-Product Relationships. *Atmos. Chem. Phys.* **2015,** *15*, 6745-6765.
23. Jokinen, T.; Sipila, M.; Richters, S.; Kerminen, V.-M.; Paasonen, P.; Stramann, F.; Worsnop, D.; Kulmala, M.; Ehn, M.; Herrmann, H.; Berndt, T., Rapid Autoxidation Forms Highly Oxidized RO_2 Radicals in the Atmosphere. *Angew. Chem. Int. Ed.* **2014,** *53*, 14596-14600.
24. Mutzel, A.; Poulain, L.; Berndt, T.; Iinuma, Y.; Rodigast, M.; Boge, O.; Richters, S.; Spindler, G.; Sipila, M.; Jokinen, T.; Kulmala, M.; Herrmann, H., Highly Oxidized Multifunctional Organic Compounds Observed in Tropospheric Particles: A Field and Laboratory Study. *Environ. Sci. Technol.* **2015,** *49*, 7754-7761.
25. Peeters, J.; Muller, J.-F.; Stavrakou, T.; Nguyen, V. S., Hydroxyl Radical Recycling in Isoprene Oxidation Driven by Hydrogen Bonding and Hydrogen Tunneling: The Upgraded LIM1 Mechanism. *J. Phys. Chem. A* **2014,** *118*, 8625-8643.
26. Crounse, J. D.; Nielsen, L. B.; Jorgensen, S.; Kjaergaard, H. G.; Wennberg, P. O., Autoxidation of Organic Compounds in the Atmosphere. *J. Phys. Chem. Lett.* **2013,** *4*, 3513-3520.
27. Wu, R.; Wang, S.; Wang, L., A New Mechanism for The Atmospheric Oxidation of Dimethyl Sulfide. The Importance of Intramolecular Hydrogen Shift in CH_3SCH_2OO Radical. *J. Phys. Chem. A* **2015,** *119*, 112-117.
28. Wang, S.; Wang, L., The Atmospheric Oxidation of Dimethyl, Diethyl, and Diisopropyl Ethers. The Role of the Intramolecular Hydrogen Shift in Peroxy Radicals. *Phys. Chem. Chem. Phys.* **2016,** *18*, 7707-7714.
29. Ehn, M.; Thornton, J. A.; Kleist, E.; Sipilä, M.; Junninen, H.; Pullinen, I.; Springer, M.; Rubach, F.; Tillmann, R.; Lee, B.; Lopez-Hilfiker, F.; Andres, S.; Acir, I.-H.; Rissanen, M.; Jokinen, T.; Schobesberger, S.; Kangasluoma, J.; Kontkanen, J.; Nieminen, T.; Kurtén, T.; Nielsen, L. B.; Jørgensen, S.; Kjaergaard, H. G.; Canagaratna, M.; Maso, M. D.; Berndt, T.; Petäjä, T.; Wahner, A.; Kerminen, V.-M.; Kulmala, M.; Worsnop, D. R.; Wildt, J.; Mentel, T. F., A Large Source of Low-Volatility Secondary Organic Aerosol. *Nature* **2014,** *506*, 476-479.
30. Molteni, U.; Bianchi, F.; Klein, F.; El Haddad, I.; Frege, C.; Rossi, M. J.; Dommen, J.; Baltensperger, U., Formation of Highly Oxygenated Organic Molecules from Aromatic Compounds. *Atmos. Chem. Phys. Discuss.* **2016**, doi:10.5194/acp-2016-1126.
31. Zhao, Y.; Truhlar, D. G., The M06 Suite of Density Functionals for Main Group Thermochemistry, Thermochemical Kinetics, Noncovalent Interactions, Excited States, and Transition Elements: Two New Functionals and Systematic Testing of Four M06-Class Functionals and 12 Other Functionals. *Theor. Chem. Acc.* **2008,** *120*, 215-241.
32. Wood, G. P. F.; Radom, L.; Petersson, G. A.; Barnes, E. C.; Frisch, M. J.; Montgomery, J., J. A., A Restricted-Open-Shell Complete-Basis-Set Model Chemistry. *J. Chem. Phys.* **2006,** *125*, 094106.
33. Jensen, F., *Introduction to Computational Chemistry*. 2nd ed.; John Wiley & Sons, Ltd: West Sussex, 2007.

34. Lee, T. J.; Taylor, P. R., A Diagnostic for Determining the Quality of Single-Reference Electron Correlation Methods. *Int. J. Quantum Chem.* **1989,** *S23*, 199-207.
35. Olivella, S.; Sole, A.; Bofill, J. M., Theoretical Mechanistic Study of the Oxidative Degradation of Benzene in the Troposphere: Reaction of Benzene-HO Radical Adduct with O_2. *J. Chem. Theory Comput.* **2009,** *5*, 1607-1623.
36. Frisch, M. J.; Trucks, G. W.; Schlegel, H. B.; Scuseria, G. E.; Robb, M. A.; Cheeseman, J. R.; Scalmani, G.; Barone, V.; Mennucci, B.; Petersson, G. A.; Nakatsuji, H.; Caricato, M.; Li, X.; Hratchian, H. P.; Izmaylov, A. F.; Bloino, J.; Zheng, G.; Sonnenberg, J. L.; Hada, M.; Ehara, M.; Toyota, K.; Fukuda, R.; Hasegawa, J.; Ishida, M.; Nakajima, T.; Honda, Y.; Kitao, O.; Nakai, H.; Vreven, T.; Montgomery, J., J. A.; Peralta, J. E.; Ogliaro, F.; Bearpark, M.; Heyd, J. J.; Brothers, E.; Kudin, K. N.; Staroverov, V. N.; Kobayashi, R.; Normand, J.; Raghavachari, K.; Rendell, A.; Burant, J. C.; Iyengar, S. S.; Tomasi, J.; Cossi, M.; Rega, N.; Millam, N. J.; Klene, M.; Knox, J. E.; Cross, J. B.; Bakken, V.; Adamo, C.; Jaramillo, J.; Gomperts, R.; Stratmann, R. E.; Yazyev, O.; Austin, A. J.; Cammi, R.; Pomelli, C.; Ochterski, J. W.; Martin, R. L.; Morokuma, K.; Zakrzewski, V. G.; Voth, G. A.; Salvador, P.; Dannenberg, J. J.; Dapprich, S.; Daniels, A. D.; Farkas, Ö.; Foresman, J. B.; Ortiz, J. V.; Cioslowski, J.; Fox, D. J. *Gaussian 09, Revision A.1*, Gaussian, Inc.: Wallingford CT, 2009.
37. Holbrook, K. A.; Pilling, M. J.; Robertson, S. H.; Robinson, P. J., *Unimolecular Reactions*. 2nd ed.; Wiley: New York, 1996.
38. Forst, W., *Unimolecular Reactions: A Concise Introduction*. Cambridge University Press: 2003.
39. Fernandez-Ramos, A.; Ellingson, B. A.; Meana-Paneda, R.; Marques, J. M. C.; Truhlar, D. G., Symmetry Number and Chemical Reaction Rates. *Theor. Chem. Acc.* **2007,** *118*, 813-826.
40. Pilling, M. J.; Seakins, P. W., *Reaction Kinetics*. Oxford University Press Inc.: New York, 1999.
41. Glowacki, D. R.; Liang, C. H.; Morley, C.; Pilling, M. J.; Robertson, S. H., MESMER: An Open-Source Master Equation Solver for Multi-Energy Well Reactions. *J. Phys. Chem. A* **2012,** *116*, 9545-9560.
42. Gilbert, R. G.; Smith, S. C., *Theory of Unimolecular and Recombination Reactions*. Blackwell Scientific Publications: Boston, 1990.
43. Miller, W. H., Tunneling Corrections to Unimolecular Rate Constants, with Application to Formaldehyde. *J. Am. Chem. Soc.* **1979,** *101*, 6810-6814.
44. Berndt, T.; Richters, S.; Jokinen, T.; Hyttinen, N.; Kurtén, T.; Otkjær, R. V.; Kjaergaard, H. G.; Stratmann, F.; Herrmann, H.; Sipilä, M.; Kulmala, M.; Ehn, M., Hydroxyl radical-induced formation of highly oxidized organic compounds. **2016,** *7*, 13677.
45. Berndt, T.; Richters, S.; Kaethner, R.; Voigtländer, J.; Stratmann, F.; Sipilä, M.; Kulmala, M.; Herrmann, H., Gas-phase Ozonolysis of Cycloalkenes: Formation of Highly Oxidized RO_2 Radicals and Their Reactions with NO, NO_2, SO_2, and Other RO_2 Radicals. *J. Phys. Chem. A* **2015,** *119*, 10336-10348.
46. Jokinen, T.; Sipilä, M.; Junninen, H.; Ehn, M.; Lonn, G.; Hakala, J.; Petäjä, T.; Mauldin, R. L. I.; Kulmala, M.; Worsnop, D. R., Atmospheric Sulphuric Acid and Neutral Cluster Measurements Using CI-APi-TOF. *Atmos. Chem. Phys.* **2012,** *12*, 4117-4125.
47. Junninen, H.; Ehn, M.; Petäjä, T.; Luosujärvi, L.; Kostiainen, R.; Rohner, U.; Gonin, M.; Fuhrer, K.; Kulmala, M.; Worsnop, D. R., A High-Resolution Mass Spectrometer to Measure Atmospheric Ion Composition. *Atmos. Meas. Tech.* **2010,** *3*, 1039-1053.

48. Li, Y.; Wang, L., The Atmospheric Oxidation Mechanism of 1,2,4-Trimethylbenzene Initiated by OH Radical. *Phys. Chem. Chem. Phys.* **2014,** *16*, 17908-17917.
49. Pan, S.; Wang, L., Atmospheric Oxidation Mechanism of *m*-Xylene Initiated by OH Radical. *J. Phys. Chem. A* **2014,** *118*, 10778-10787.
50. Wang, L.; Wu, R.; Xu, C., Atmospheric Oxidation Mechanism of Benzene. Fates of Alkoxy Radical Intermediates and Revised Mechanism. *J. Phys. Chem. A* **2013,** *117*, 14163-14168.
51. Pan, S.; Wang, L., The Atmospheric Oxidation Mechanism of *o*-Xylene Initiated by Hydroxyl Radicals. *Acta Phys. -Chim. Sin.* **2015,** *31*, 2295-2268.
52. Orlando, J. J.; Tyndall, G. S., Laboratory Studies of Organic Peroxy Radical Chemistry: An Overview with Emphasis on Recent Issues of Atmospheric Significance. *Chem. Soc. Rev.* **2012,** *41*, 6294-6317.
53. Hofzumahaus, A.; Rohrer, F.; Lu, K.; Bohn, B.; Brauers, T.; Chang, C.-C.; Fuchs, H.; Holland, F.; Kita, K.; Kondo, Y.; Li, X.; Lou, S.; Shao, M.; Zeng, L.; Wahner, A.; Zhang, Y., Amplified Trace Gas Removal in the Troposphere. *Science* **2009,** *324*, 1702-1704.
54. Wine, P. H.; Astalos, R. J.; Mauldin, R. L. I., Kinetic and Mechanistic Study of the Hydroxyl + Formic Acid Reaction. *J. Phys. Chem.* **1985,** *89*, 2620-2624.
55. Hyttinen, N.; Rissanen, M.; Kurtén, T., Computational Comparison of Acetate and Nitrate Chemical Ionization of Highly Oxidized Cyclohexene Ozonolysis Intermediates and Products. *J. Phys. Chem. A* **2017,** *121*, 2172-2179.